THEORETICAL AND EXPERIMENTAL INVESTIGATIONS OF VELOCITY DISTRIBUTIONS FOR ROUND JETS

By Il Won Seo[1], Mohamed S. Gadalrab[2], Siwan Lyu[2], and Yongsung Park[3]

[1] Assoc. Prof., Dept. of Civil Engineering, Seoul National Univ., Seoul, Korea
[2] Grad. Student, Dept. of Civil Engineering, Seoul National Univ., Seoul, Korea
[3] Researcher, N4Tech Water Co., Ltd., Anyang, Korea

Abstract: The theoretical treatments on jets, in which the flow is issuing into a stagnant medium, have been based on Prandtl's mixing theory. In this study, using Prandtl's mixing length hypothesis, a theoretical relationship for the velocity profile of a single round jet is derived. Furthermore, Gaussian expression is used to approximate the theoretical relationship, in which the Gaussian coefficient is assumed to be decreasing exponentially as the flow goes far from the orifice. Two data sets for a single round jet performed by two different techniques of measurement are used to verify the suggested relationships. The theoretical and Gaussian distributions give close results in spite of the difference in approach. The observed mean velocity distributions are in good agreements with the suggested theoretical and Gaussian distributions.

Keywords: round jet, velocity distribution, theoretical distributions, Gaussian approximation, experiments

1. INTRODUCTION

The first analysis of turbulent jet mixing of incompressible fluids was done by Tollmien (1926) by application of Prandtl's mixing length theory. He solved the following problems: mixing of a two-dimensional jet issuing from a very narrow opening with a medium at rest; and mixing of an axially symmetric jet escaping from a very small opening with a medium at rest. Reichardt (1942), from the experimental data, suggested an inductive theory, which corresponds essentially to a constant exchange coefficient over the mixing zone for the free turbulence problem. Gortler (1942) reexamined Tollmien's problems by the application of Reichardt's assumption with some suggestions from Prandtl, and obtained some improvements in the velocity profiles in the jet.

An observer of the jet flow can notice that the mean velocity exhibits a self-similarity and a typical bell-shaped velocity distribution that is well approximated by the Gaussian profile, Fig. 1. The Gaussian distribution is in good agreement with experimental data at some distance from the point of release, i.e., the zone of fully developed flow (Davidson et al., 1993; Larsen, 1993; and Chu et al., 1999). This agreement can be explained from the nature of the phenomenon itself, i.e., turbulence is mainly random motion and the Gaussian distribution also represent random phenomena, or it may be simply that velocities tend to concentrate around its mean values, which yields normal distribution so that the Gaussian curve can fit them well. However, a theoretical base is needed to obtain the best and universal Gaussian fit of velocity distribution.

In this paper, we look more closely at the classical jet equations based on Prandtl's hypothesis. In particular, we attempt to derive a new equation representing the velocity distribution for round jets based on the Gaussian distribution as well as the theoretical expressions derived using the mixing length theory. Two sets of experiments are used to verify the derived equations. The first data set was performed by Yu et al. (1998) and the velocities were measured using an acoustic Doppler velocimeter for single jet discharged into stagnant water. A special experimental set-up was conducted for a single jet discharging water through a stagnant water ambient with different values of relative density. Flow velocities were collected using particle image velocimetry. Finally, we try to answer the following question: Can a velocity distribution for a round jet be represented by a single Gaussian curve?

2. VELOCITY DISTRIBUTIONS

2.1 Theoretical Solution

Let us consider a circular jet of diameter d_p emerging from a nozzle with a uniform velocity of U_o into a large stagnant mass of the same fluid, as shown in Fig. 1. If we observe the jet, we would find that the size of the jet increases steadily as it travels away from the nozzle. At the end of the flow development region, the core velocity is equal to U_o, the turbulence generated on the boundaries penetrates to the axis, and the mean velocity on the axis begins to decay with distance. In the region of fully developed flow, we find that at any section velocity decreases continuously from a maximum value on the axis to zero for large values of the radius. The velocity distributions at different distances from the nozzle appear to have the same shape. It has been experimentally found that the velocity distribution could be presented satisfactorily by a Gaussian curve.

In the mixing length theory, Prandtl assumed that both the longitudinal and the transverse turbulent fluctuating velocities are proportional to the transverse mean velocity gradient. We write

$$u' \sim v' \sim l \, \frac{\partial \bar{u}}{\partial r} \tag{1}$$

where $\bar{u}$ is the mean velocity in the z-direction, i.e., the main flow directions; l is the mixing length; and u' and v' are the z- and r- components of the fluctuating velocity, respectively. The rate of increase of the width, b, of the mixing zone with respect to time is comparable with the fluctuating velocity component across the flow. If we replace the mean value of $\frac{\partial \bar{u}}{\partial r}$ as a first approximation by U/b, where U is the maximum velocity at the axis of the jet in the mixing region, we then have

$$\frac{Db}{Dt} \propto \frac{l}{b} U \tag{2}$$

The first assumption in Tollmien's theory of free turbulent flow is that l/b is assumed to be constant across a given section of the mixing region. Since

$$\frac{Db}{Dt} = (constant)\ U\ \frac{db}{dz} \tag{3}$$

For steady flow, we have

$$\frac{db}{dz} = constant \tag{4a}$$

$$b = C_1 z + C_2 \tag{4b}$$

where C_1 and C_2 are constants. Eq. (4) shows that the spread of a turbulent jet increases linearly with z, the distance along the axis of the jet.

The equation of motion in cylindrical coordinates is

$$v\ \frac{\partial v}{\partial r} + u\ \frac{\partial u}{\partial z} = \frac{1}{\rho\ r}\frac{\partial r\ \tau}{\partial r} \tag{5}$$

where ρ is the fluid density and τ is the shear stress. The equivalent expression for the kinematic momentum, K, in the z-direction is

$$K = \frac{J}{\rho} = 2\ \pi \int_0^{\infty} \bar{u}^2\ r\,dr = constant \tag{6}$$

where J is the momentum flux. The eddy viscosity, ε, is assumed to be constant throughout the mixing region of the jet. The equation of motion becomes

$$\bar{v}\ \frac{\partial \bar{v}}{\partial r} + \bar{u}\ \frac{\partial \bar{u}}{\partial z} = \frac{\varepsilon}{r}\frac{\partial}{\partial r}\left(r\ \frac{\partial \bar{u}}{\partial r}\right) \tag{7}$$

The pressure gradient can be neglected because the constant pressure in the surrounding fluid impresses itself on the jet. Prandtl's hypothesis leads to

$$u\ \frac{\partial u}{\partial z} + v\ \frac{\partial v}{\partial r} = \varepsilon\ \frac{\partial^2 u}{\partial r^2} \tag{8}$$

The continuity equation is

$$\frac{1}{r}\ \frac{\partial}{\partial r}\ (\ r\ v\ ) + \frac{\partial}{\partial z}\ (\ r\ u\ ) = 0 \tag{9}$$

The width of the jet will be taken to be proportional to z^n, it being further assumed that the stream function $\psi \sim z^p\ F(\eta)$ with $\eta = r/z^n$. The exponents p and n will be determined from the conditions of constant kinematic momentum and the inertia, and frictional terms in the equation of motion must be of the same order of magnitude, so that, $p = n = 1$. Consequently, we may now put

$$\psi = \varepsilon\ z\ F(\ \eta\ ) \tag{10}$$

And the velocity components are

$$u = -\frac{\partial \psi}{\partial r} = \frac{\varepsilon}{z}\frac{F'}{\eta} \tag{11}$$

$$v = \frac{\partial \psi}{\partial z} = \frac{\varepsilon}{z}\left(F' - \frac{F}{\eta}\right) \tag{12}$$

Inserting Eqs. (11)-(12) into the equation of motion, Eq. (8), we obtain

$$\frac{F\ F'}{\eta^2} - \frac{F'^{\,2}}{\eta} - \frac{F\ F''}{\eta} = \frac{d}{d\ \eta}\left(F'' - \frac{F'}{\eta}\right) \tag{13}$$

Integrate once

$$F\ F' = F' - \eta\ F'' \tag{14}$$

If $F(\eta)$ is a solution of the above equation, then $F(m\ \eta) = F(\xi)$, where m is a constant of integration, is also a solution of the differential equation, which satisfies the boundary condition: $F = 0$, $F_o = 0$ at $\xi = 0$,

$$F \frac{dF}{d\xi} = \frac{dF}{d\xi} - \xi \frac{d^2F}{d\xi^2} \tag{15}$$

Integrating once and using the boundary conditions,

$$\xi F' - 2F + \frac{1}{2} F^2 = 0 \tag{16}$$

A particular solution of Eq. (16) is given by

$$F = \frac{\xi^2}{1 + \frac{1}{4}\xi^2} \tag{17}$$

Hence, we obtain Eq. (18) from Eq. (11)

$$u = \frac{\varepsilon}{z} \frac{2m^2}{1 + \frac{1}{4}\xi^2} \tag{18}$$

From Eq. (6), we obtain

$$K = 2\pi \int_0^\infty u^2 r\, dr = \frac{16}{3} \pi m^2 \varepsilon^2 \tag{19}$$

Finally, the above results can be expressed as

$$u = \frac{3}{8\pi} \frac{K}{\varepsilon z} \frac{1}{\left(1 + \frac{1}{4}\xi^2\right)^2} \tag{20}$$

$$\xi = \frac{1}{4} \sqrt{\frac{3}{\pi}} \frac{\sqrt{K}}{\varepsilon} \frac{r}{z} \tag{21}$$

Now, the empirical constant is equal to $m = \sqrt{K} / \varepsilon$. According to the measurement performed by Reichardt, the width of the jet is given by

$$b = 0.0848\, z \tag{22a}$$

$$\xi = 1.286 \quad \text{at } u = 1/2U \tag{22b}$$

Substituting the preceding value of ξ into Eq. (21), we get

$$b = 5.27 z\varepsilon / \sqrt{K} \tag{23}$$

Equating the preceding two values of b, we get $\varepsilon / \sqrt{K} = 0.0161$. Substituting this into Eq. (20) using $u = 1/2U$ as well as Reichardt results' of b and ξ, we get

$$\sqrt{K} = 1.59\, b\, U \tag{24}$$

Finally, we can rewrite Eq. (20) as follows

$$\frac{u}{U} = \frac{1}{\left[1 + 58\left(\frac{r}{z}\right)^2\right]^2} \tag{25}$$

The above equation has the same form as that of Daily and Harelman's (1966) equation in spite of the fact that their approach is different from the theoretical method proposed in this study. The theoretical equation derived by Daily and Harelman (1966) is given as

$$\frac{u}{U} = \frac{1}{\left[1 + 62.5\left(\frac{r}{z}\right)^2\right]^2} \tag{26}$$

2.2 Gaussian Approximation

In the fully developed flow region, the transverse distribution of the mean velocity in the z-direction, i.e. the variation of u with r at different sections, has the same geometrical shape as shown in Fig. 1. At every section, u decreases continuously from the maximum value of U on the axis to zero at some distance from the axis.

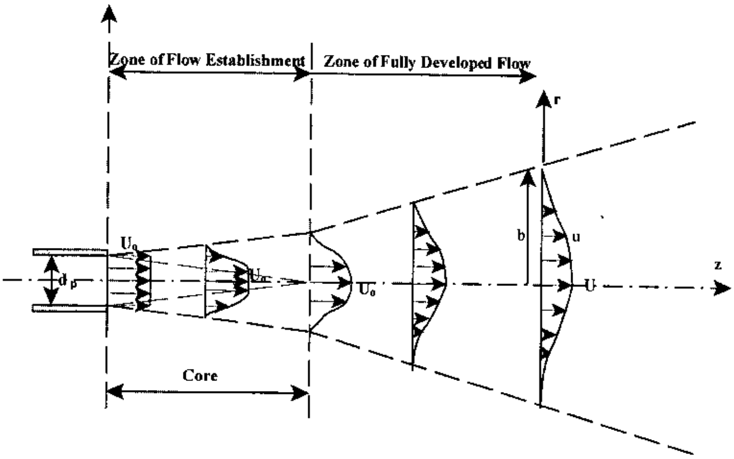

Fig. 1. Development of Similar Velocity in a Round Jet

Let us now try to compare the distributions at different sections in a dimensionless form. At each section, let us make the velocity u dimensionless by dividing it by U at that section and plot u/U against r/z. We will find that the velocity distributions at different sections fall on one common curve. The velocity profiles at different sections that can be superposed in this manner are said to be similar (Pani and Dash, 1983; Rajaratnam, 1967).

An essential characteristic of turbulent motion is that the turbulent fluctuations are random in nature. Hence the final and logical solution of the turbulent flow problem requires the application of methods of statistical mechanics. During the initial phases of the jet flow the velocity distribution will be dominant by the issuing velocity but the velocity will always decrease gradually with time and asymptotically the distribution will become Gaussian. This assumption is necessary in order to obtain the distribution. A typical velocity distribution across the jets and plumes is closely approximated by Gaussian profiles as follows

$$\frac{u}{U} = \exp\left[-c\left(\frac{r}{z}\right)^2\right] \tag{27}$$

here c is an arbitrary constant.

A number of investigators suggested different values for c based on their experimental results. A few of them are listed in Table 1. As shown in this table, values for c vary in quite a large range. Thus, in this study, in order to get the best value of the parameter c, the Gaussian equation is fitted to the theoretical distribution. Fig. 2 shows the relation between the parameter c vs. the dimensionless distance r/z, where it is clear that c decreases as r/z increases. The parameter c is varied exponentially with respect to r/z. It has been found that the parameter is given by

Table 1. Different Values of Gaussian Coefficients

Investigator	c
Reichardt (1951)	48
Sohlichting (1979)	72
Yu et al. (1998)	78
Hinze (1959)	108

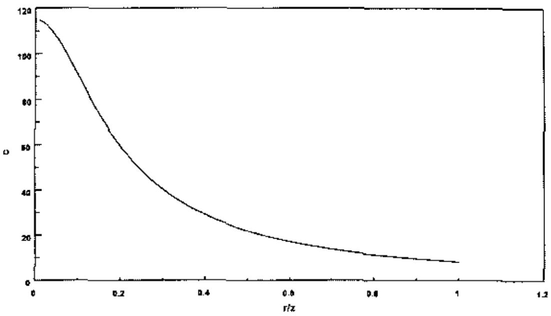

Fig. 2. Variation of Gaussian Distributions' Parameter, c

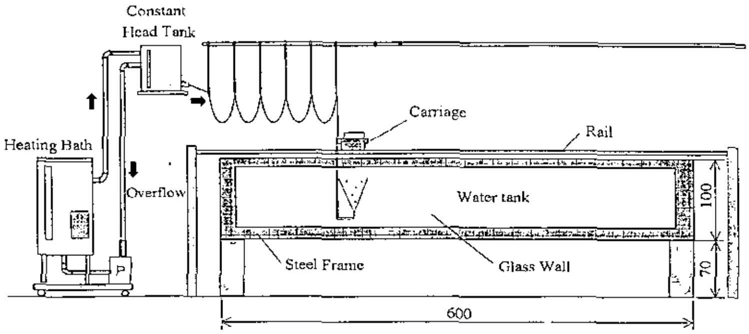

Fig. 3. Experimental Setup (unit : cm)

$$c = \exp\left[-2.75 * \left(\frac{r}{z}\right) + 4.61 \right] \tag{28}$$

Hence, the suggested Gaussian velocity profile can be written as

$$\frac{u}{U} = \exp\left[-\exp\left[-2.75 * \left(\frac{r}{z}\right) + 4.61 \right] * \left(\frac{r}{z}\right)^2 \right] \tag{29}$$

3. EXPERIMENTAL INVESTIGATIONS

In order to test the applicability of the derived equation, it was necessary to devise an experimental configuration where the ambient water is stagnant. The experimental set-up is illustrated in Fig. 3. The experiments were carried out in a glass-walled tank 6.0 m by 1.2 m in cross section and 0.8 m deep, filled with freshwater to a depth of nearly 0.7 m. Heated water was discharged through a circular nozzle 10 mm in diameter set near the bottom of the freshwater tank. Supply tank was provided with a boiler so that the heated water could be injected into the freshwater tank through a main control valve. The supply of heated water was turned on and flowed at a constant rate and temperature throughout the run. Five cases of experiments were performed to measure the velocity distribution at various distances from the nozzle through the investigated area. Table 2 shows the data sets and variation of parameters.

Flow visualization and particle image velocimetry (PIV) were used to investigate the jet flow in a longitudinal cross-section. Fig. 4

Table 2. Initial Parameters of Experiments

Case	H (cm)	T_o (°C)	T_a (°C)	$g'_o = g \cdot \frac{\Delta\rho_o}{e}$ (m/s²)	U_o (m/s)	$Fr_j = g \cdot \frac{U_o}{\sqrt{g'_o d_p}}$	$Re = \frac{U_o d_p}{\nu}$
VJ101	67.3	20	12.12	0.012	0.567	48.2	5484
VJ102	67.3	25	12.22	0.023	0.531	35.0	6137
VJ103	67.3	30	12.30	0.035	0.509	31.3	6656
VJ104	67.5	35	14.17	0.052	0.587	24.7	7632
VJ105	67.5	40	14.95	0.069	0.506	19.8	7842

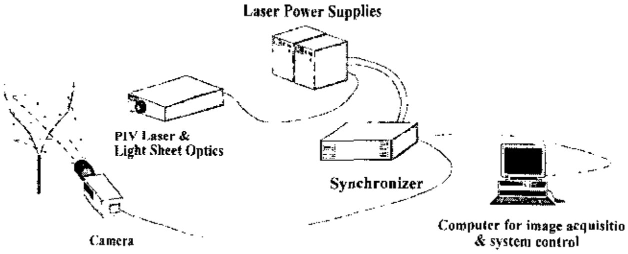

Fig. 4. Schematic Diagram of PIV System

shows the set up of the PIV system. A light sheet from a 32 mJ/pulse Nd-YAG laser was used to illuminate a plane through the centerline of the nozzle, and the dyed jet was recorded on a computer. PIV experiments were performed using a TSI Particle Image Velocimetry system based on cross-correlating pairs of images to avoid directional ambiguity. A Kodak Megaplus ES 1.0 CCD camera (1016×1008 pixel resolution) positioned perpendicular to the light sheet was used to capture the images in a 27.02(H) ×27.45(V) cm region of the flow. The jet liquid was seeded with hollow glass spheres (mean diameter: 8 ~ 12 μm, specific gravity : 0.1 ~ 1.5 g/cc). Based on an analysis by Raffel et al. (1998), these particles will follow the fluid motion for velocity fluctuations at a significantly higher frequency than those encountered in the flow.

The images were obtained in planes parallel to the jet axis at 30 Hz for 2 seconds. *INSIGHT* software from TSI was used to process the images. Among the measuring schemes provided by *INSIGHT* software, the 2-frame cross-correlation technique was applied. During the processing, each image is sub-sampled into smaller windows called interrogation spots and the velocity is measured within each zone by performing a cross-correlation with a zone in a subsequent image. The location of the cross-correlation peak with respect to the origin in correlation space determines the average particle displacement within the interrogation zone from one image to the next. Dividing by the time between images yields the mean velocity.

Besides the experimental data obtained in this study, velocity data collected by Yu et al. (1998) were also used to verify the theoretical relations. Yu et al. (1998) performed laboratory experiments on vertical jets discharged into stagnant water. In their experiments, both fresh water and heated water were used as the discharging fluid.

Table 3. Experimental Parameters of Vertical Jet Experiments by Yu et al. (1998)

Case	H (cm)	ΔT_o (°C)	U_o (m/s)	Initial Volume Flux (cm^3/s)	Initial Momentum Flux (cm^4/s^2)	Initial Buoyancy Flux (cm^4/s^3)	$Fr_j = g \cdot \frac{U_o}{\sqrt{g'_o d_p}}$
SJ1	45	0.0	0.85	66.8	5674.5	0.0	
SJ2	45	10.7	0.85	66.8	5674.5	142.3	58.2
SJ3	45	16.3	0.17	133.5	22698.0	529.7	85.3
SJ4	25	18.5	0.34	267.0	90792.0	1258.8	156.6

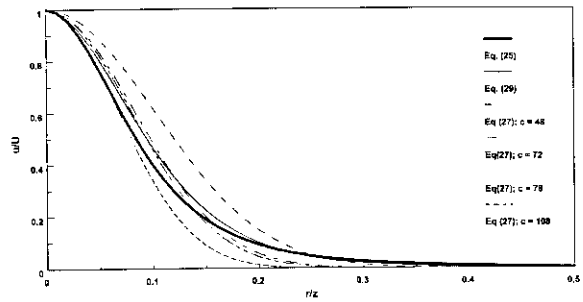

Fig. 5. Theoretical and Gaussian Distributions

The jet nozzle was 4.3 mm in diameter, and set near the bottom of the freshwater tank of which the dimensions were 4.9×15.5×0.6m. In measuring the velocity of the single jet, they used the acoustic Doppler velocimeter (ADV). Experimental parameters are illustrated in Table 3.

4. ANALYSIS OF RESULTS

Fig. 5 shows the theoretical relationship, Eq. (25), and proposed Gaussian equation, Eq. (29) as well as the other Gaussian curves with the coefficients listed in Table 1. As shown in this figure, the Gaussian curve with the coefficient proposed in this study, Eq. (29), fits the theoretical equation quite well throughout the whole extent of r/z. The Gaussian curve with the coefficient proposed in this study is slightly high up to 0.2 r/z and then coincides perfectly with the theoretical curve. However, Gaussian curves, Eq. (27) with coefficients of single constant values given in Table 1 either overestimate or underestimate. Among the coefficients given in Table 1, c = 72~78 give the reasonable fit to the theoretical curve even though these Gaussian curves have tendency, near the center of the jet, to overshoot the theoretical curve and undershoot the theoretical curve at the wing side of the jet. Daily and Harleman (1966) also maintained that, at both center and wing side of the round jet, Gaussian curves with single constants give velocity distributions which are different than those by experiments and the theoretical solution. This is simply because Gaussian curve is the only approximation of the theoretical solution, in which equations of motion and continuity are solved analytically for the velocity distribution of the jet.

The lateral velocity distributions at different

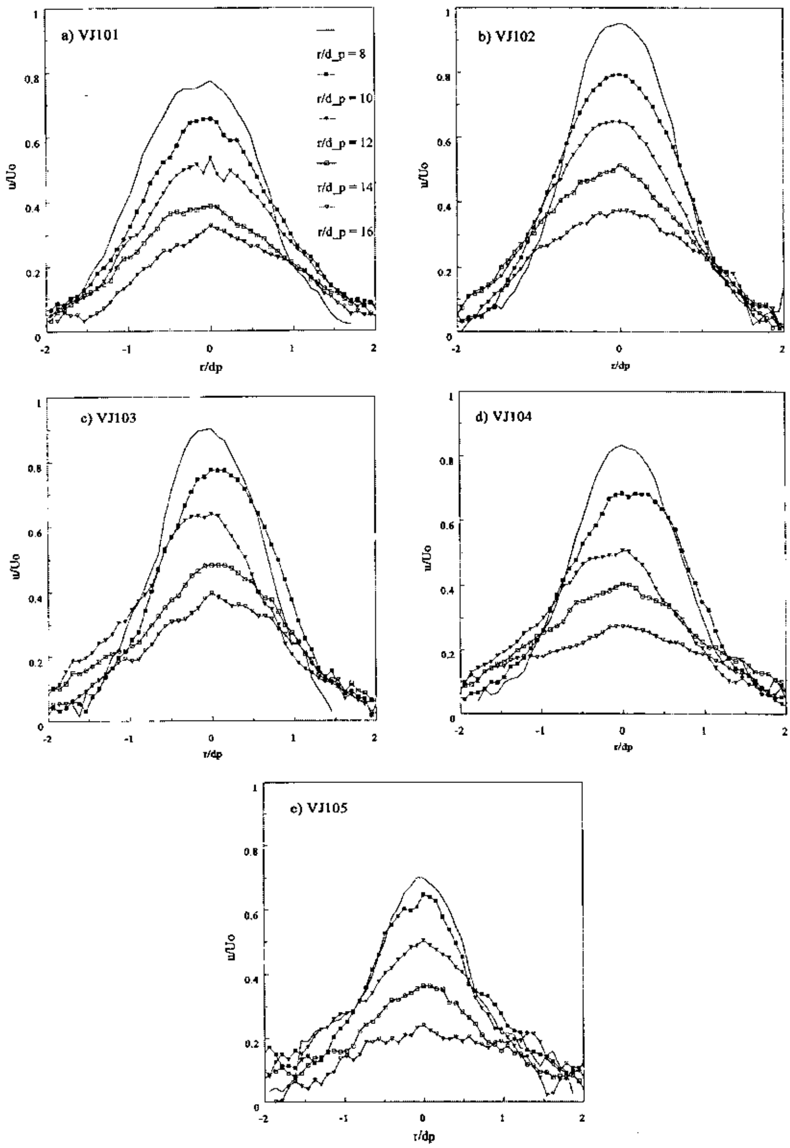

Fig. 6. Lateral Velocity Distributions for Each Case

axial distances for each case are shown in Fig. 6. In these figures, velocity profiles are similar. The velocity profiles tend to follow Gaussian distribution from the beginning of the zone of established flow. The longitudinal variations of jet width against the axial distance for each case are shown in Fig. 7. In this figure, b is the value of r where u is equal to 1/e of the maximum velocity at the jet axis. The jet width b is specified by the function of the form as

$$\frac{b}{d_p} = f\left(\frac{z}{d_p}\right) + const \tag{30}$$

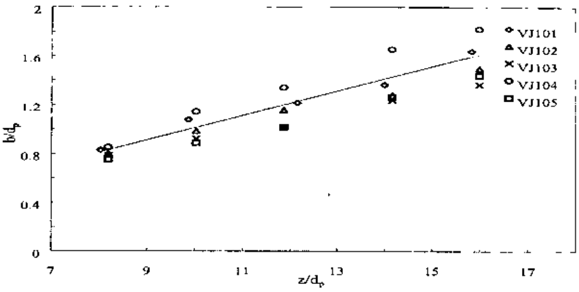

Fig. 7. Variation of Jet Width

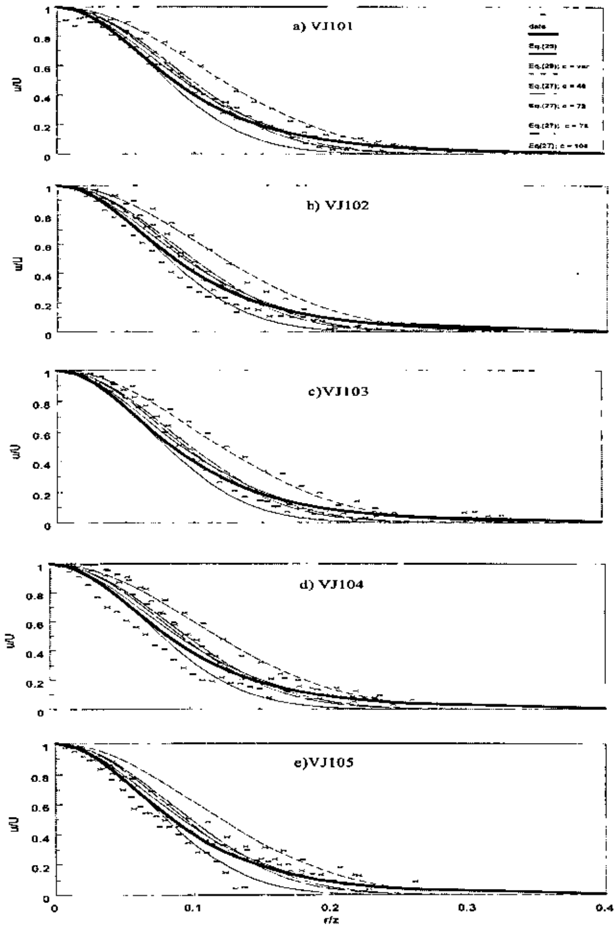

Fig. 8. Comparison Among Theoretical Solution and Different Gaussian Forms for PIV Data

A number of experimental investigations (Fischer et al., 1979) involving a single round jet show that length scale *b* of a single jet is linear to the longitudinal distance. They postulated that the average value of *b/z*, referred to the width parameter, is 0.107. Here, in this study, average value of *b/z*, which is the slope of the linear equation plotted in Fig. 7, is 0.10.

Figs. 8 and 9 show a graph of dimensionless velocity against the dimensionless distance from

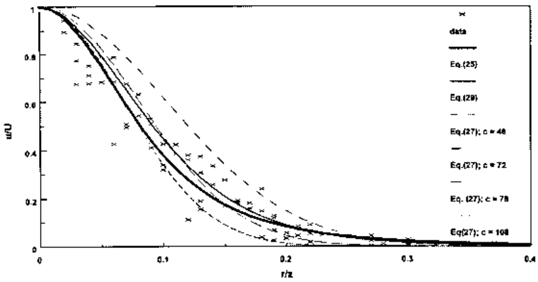

Fig. 9. Comparisons Among Theoretical Solution and Different Gaussian Forms for ADV Data

the jet orifice, *r/z*, for theoretical and Gaussian distributions as well as the experimental data of this study and Seo et al. (1998). Both the theoretical equation, Eq. (25), and proposed Gaussian curve, Eq. (29), give good agreements with the experimental data across the entire jet width. The Gaussian curve, Eq. (27), with $c = 48$ overestimates whereas the Gaussian curve with $c = 108$ underestimates. As mentioned earlier, among the coefficients given in Table 1, $c = 72 \sim 78$ give the reasonable fit to the experimental data. Table 4 shows RMS values for the theoretical and different Gaussian solutions. It is clear that the minimum error among Gaussian distributions is given by Eq. (29).

5. CONCLUSIONS

With the purpose of examining the velocity distribution in a single round jet, this paper has discussed the results from laboratory experiments to verify the theoretical relation of the mixing length theory and the Gaussian distributions. The most significant conclusion that can be drawn from this study is that the Gaussian equation may provide a valuable and accurate feature of the velocity distribution if we consider the fact that the parameter *c* in the Gaussian equation is a function of dimensionless distance, *r/z*. In other words, instead of a constant value of *c* we should apply Gaussian distribution with a varying coefficient with respect to *r/z*. Comparisons between theoretical and Gaussian equations and experimental results reveal that both the theoretical equation and the Gaussian curve with a varying coefficient proposed in this study give good agreements across the entire jet width. The Gaussian curve with c = 48 overestimates whereas the Gaussian curve with c = 108 underestimates. Among the coefficients given by previous investigators, Gaussian curves

Table 4. RMS Errors of Different Distributions

Cases	Theoretical Sol.	Gaussian Distributions				
		Variable c	c = 48	c = 72	c = 78	c = 108
VJ101	0.077	0.078	0.104	0.084	0.087	0.088
VJ102	0.094	0.096	0.127	0.115	0.097	0.091
VJ103	0.104	0.108	0.138	0.101	0.112	0.105
VJ104	0.086	0.086	0.107	0.091	0.089	0.092
VJ105	0.12	0.12	0.128	0.129	0.131	0.138

with c = 72~78 give the reasonable fit to the experimental data.

ACKNOWLEDGEMENTS

This research work was partially supported by the Environmental Technology R&D project (G-7 Project) of the Ministry of Environment and the Brain Korean 21 Project of the Ministry of Education, Korea. This research work has been conducted in the Research Institute of Engineering Science of Seoul National University, Seoul, Korea.

REFERENCES

Chu, P. C. K., Lee, J. H., and Chu, V. H. (1999). Spreading of turbulent round jet in co-flow. *J. Hyd. Engrg.*, ASCE, 125(2), 193-204.

Daily, J. W. and Harleman, D. R. F. (1966). *Fluid Dynamics*, Addison-Wesley Publishing Company, INC., New York.

Davidson, M. J., Papps, D. A., and Wood, I. R. (1993). The behaviour of merging buoyant jets. *Recent research advances in the fluid mechanics of turbulent jets and plumes*, NATO ASI Series E: Applied sciences, Vol. 255, P. A. Davies, and M. J. Valente Neves, eds., Kluwer, Dordrecht, The Netherlands, 465-478.

Fischer, B. H., List, E. J., Koh, R. C. Y., Imberger, J., and Brooks, N. H. (1979). *Mixing in inland and coastal waters*. Academic Press, Inc., New York, N.Y.

Gortler, H. (1942). Berechnung von aufgaben der freien turbulenz auf grund eines neuen naherungsansatzes. *ZAMM 22*, 244-254.

Hinze, J. O. (1959). *Turbulence*, McGraw-Hill Book Co., New York.

Larsen T. (1993). Numerical modelling of jets and plumes - A civil engineering perspective. *Recent research advances in the fluid mechanics of turbulent jets and plumes*, NATO ASI Series E: Applied sciences, Vol. 255, P. A. Davies, and M. J. Valente Neves, eds., Kluwer, Dordrecht, The Netherlands, 237-259.

Pani, B., and Dash, R. (1983). Three dimensional single and multiple free jets. *J. Hyd. Engrg.*, ASCE, 109(2), 254-269.

Raffel, M., Willert, C., and Kompenhans, J. (1998). Particle Image Velocimtry. Springer-Verlag, Berlin, Germany.

Rajaratnam, N. (1976). *Turbulent Jets*, Elsevier Scientific Publishing Company.

Reichardt, H. (1942). *Gesetzmassigkeiten der freien turbulenz*, VDI-Forschungsheft 414.

Schlicting, H. (1979). *Boundary layer theory*, 7th ed., McGraw-Hill Book Co., New York.

Tollmien, W. (1926). Berechnung turbulenter ausbreiungsvrgange. *ZAMM 6*, 468-478.

Yu, D. Y., Kim, H. S., and Seo, I. W. (1998). Velocity and dilution of the single jet discharged into stagnant water. *Third Korea-Japan bilateral symposium on water resources and environmental research*, Korean Federation of Science and Technology Societies, Seoul, Korea, 297-302.

NOTATIONS

The following symbols are used in this paper:

b = half width of the jet flow;

C_1 & C_2 = constants;

c = Gaussian parameter;

H = water depth;

d_p = jet diameter;

F = dimensionless velocity function;

Fr_j = densimetric Froude number;

g = gravitational acceleration;

g_0' = effective gravitational acceleration;

J = flux of momentum;

K = kinematic momentum;
l = mixing length;
m = constant;
p and n = exponents;
Re_j = jet Reynolds number;
r = coordinate perpendicular to the flow direction for cylindrical system;
T = temperature;
T_o = jet issuing temperature;
t = time;
U = maximum velocity at the jet axis;
U_o = jet issuing velocity;
u = component of the velocity in the direction concentric with the centerline of the jet;
v = component of the velocity in the direction perpendicular to the centerline of the jet;
z = coordinate in the flow direction for cylindrical system;
η & ξ = dimensionless distance;
ρ = density;
τ = shear stress;
ψ = stream function; and
ε = eddy viscosity.

Il Won Seo, Assoc. Prof., Dept. of Civil Engineering, Seoul National Univ., San 56-1, Shillim-Dong, Kwanak-Gu, Seoul 151-742, Korea. (E-mail: seoilwon@plaza.snu.ac.kr)

Mohamed S. Gadalrab, Grad. Student, Dept. of Civil Engineering, Seoul National Univ., San 56-1, Shillim-Dong, Kwanak-Gu, Seoul 151-742, Korea.

Siwan Lyu, Grad. Student, Dept. of Civil Engineering, Seoul National Univ., San 56-1, Shillim-Dong, Kwanak-Gu, Seoul, 151-742, Korea.

Yongsung Park, Researcher, N4Tech Water Co., Ltd., 1048-2 Hoke-Dong, Dongan-Gu, Anyang, Kyunggi-Do 431-080, Korea.

(Received October 20, 2000; accepted March 7, 2001)